Electronic Supplementary Material (ESI) for Faraday Discussions.

Plasmon-Driven Methanol Oxidation on PtAg Nanoalloys Prepared by Improved Pulsed Laser Deposition

Junpeng Wang[a], Longfei Guo[a], Bowei Pan[a], Tao Jin[a], Zhen Li[a], Quan Tang[a], Pascal Andreazza[b], Yu Chen[c], Liang An[d], Fuyi Chen[a]*

a. State Key Laboratory of Solidification Processing, Northwestern Polytechnical University, Xian, 710072, China. E-mail: fuyichen@nwpu.edu.cn

b. Interfaces, Confinement, Matériaux et Nanostructures, ICMN, Université d'Orléans, CNRS, Orléans, France

c. Department of Physics, University of Strathclyde, John Anderson Building, 107 Rottenrow, Glasgow G4 0NG, UK

d. Department of Mechanical Engineering, The Hong Kong Polytechnic University, Hung Hom, Kowloon, Hong Kong SAR, China

Supporting Information

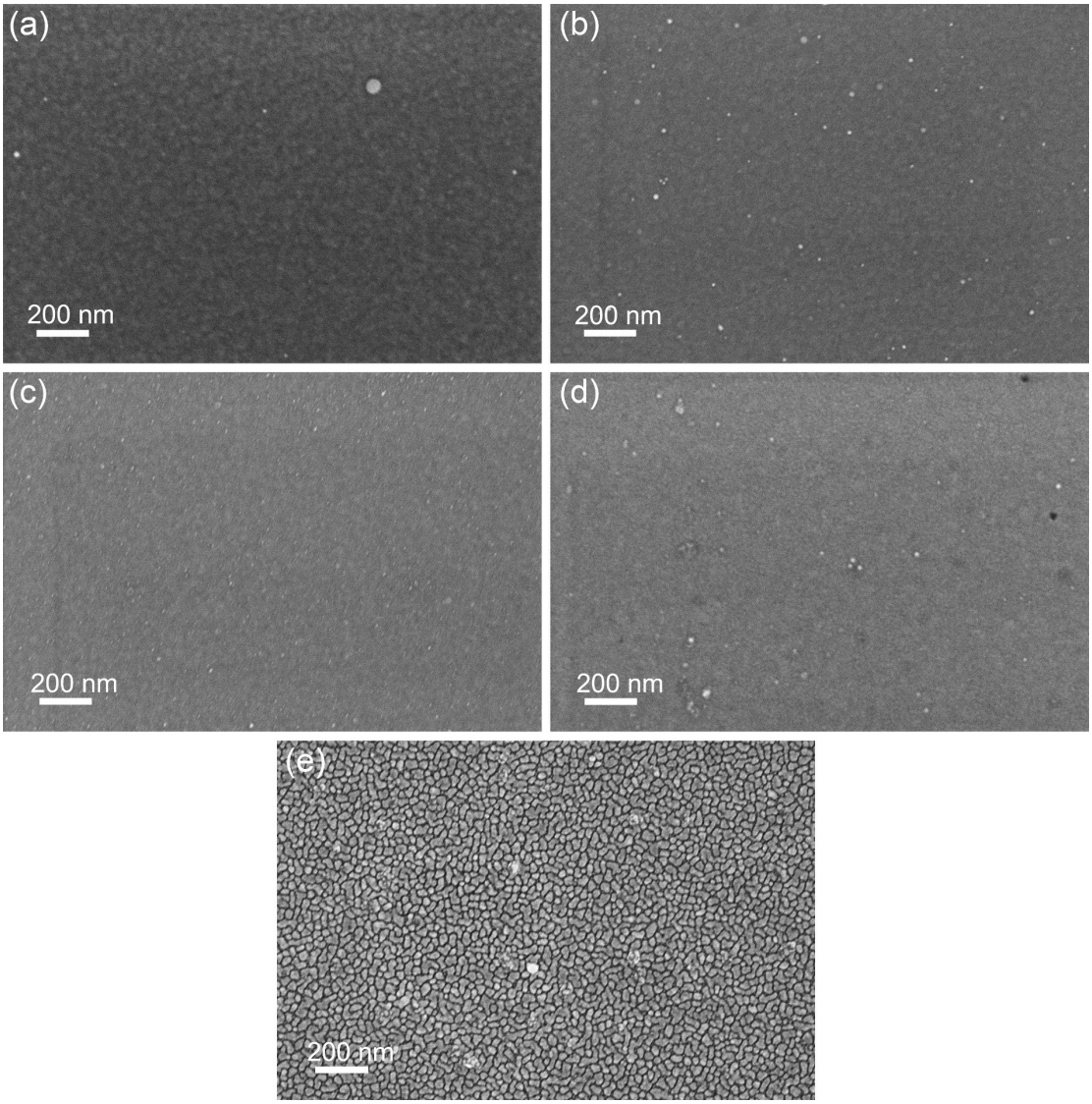

Figure S1. Morphology characterization of as-prepared samples. SEM images of Pt NP (a), $Pt_{75}Ag_{25}$ NP (b), $Pt_{50}Ag_{50}$ NP (c), $Pt_{25}Ag_{75}$ NP (d), and Ag NP (e).

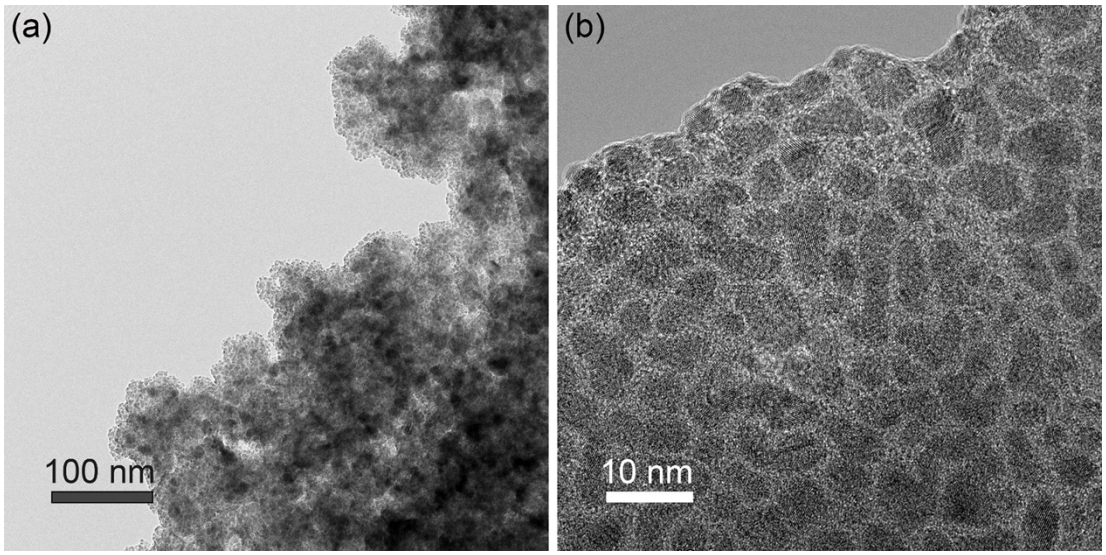

Figure S 2(a) Bright-field TEM images of $Pt_{50}Ag_{50}$ nanoparticles. (b) TEM images of $Pt_{50}Ag_{50}$ nanoparticles.

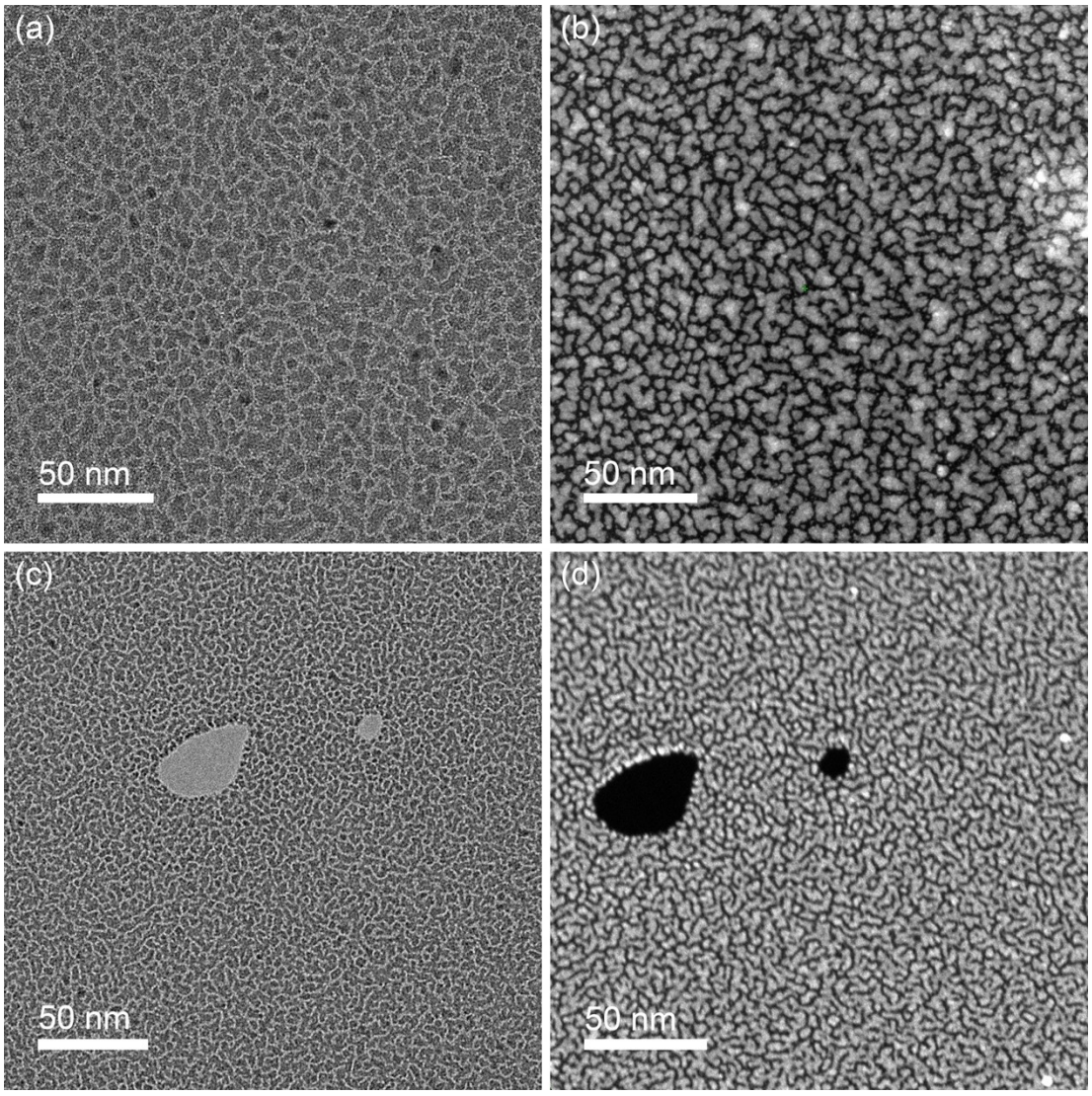

Figure S 3 (a) STEM images of $Pt_{50}Ag_{50}$ NP. (b) HAADF-STEM image of $Pt_{50}Ag_{50}$ NP. (c) STEM images of $Pt_{25}Ag_{75}$ NP. (d) HAADF-STEM image of $Pt_{25}Ag_{75}$ NP.

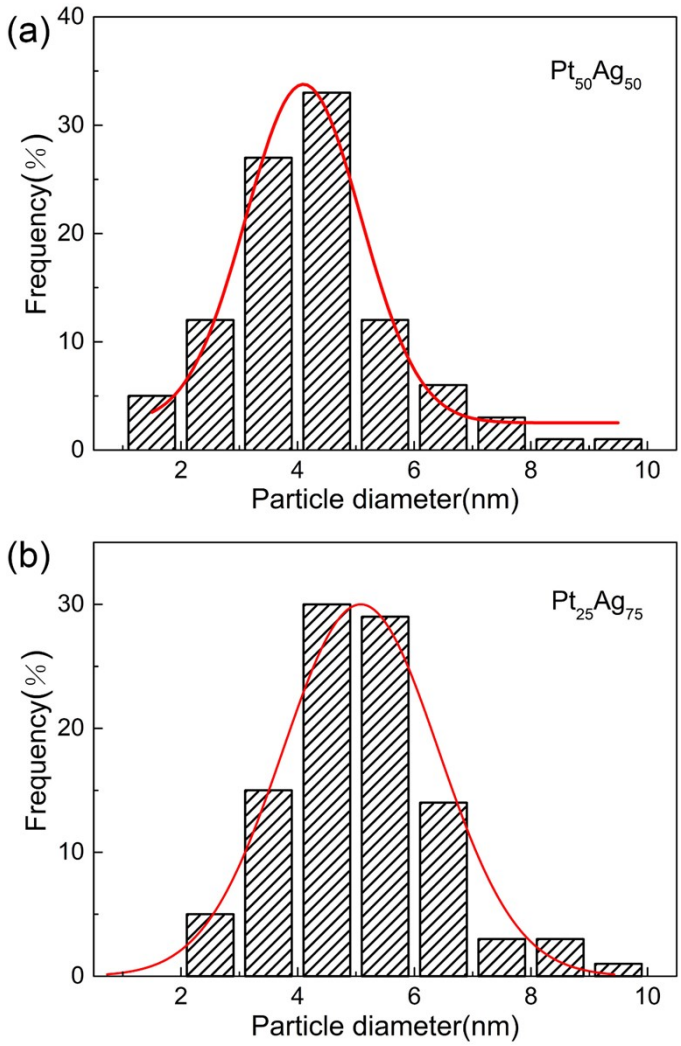

Figure S 4 Particle size distribution of as-prepared samples corresponding to Fig-S3. (a) $Pt_{50}Ag_{50}$ NP, (b) $Pt_{25}Ag_{75}$ NP.

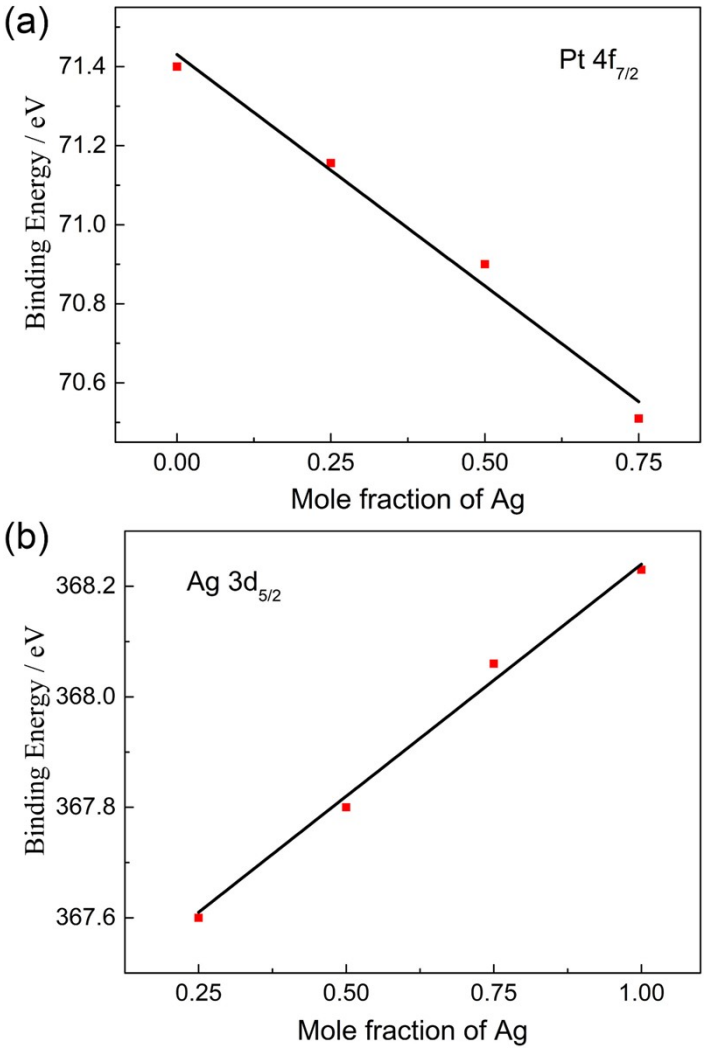

Figure S 5(a, b) Plot of the binding energy of Pt 4f $_{7/2}$ and Ag $3d_{5/2}$ versus the Ag mole fraction in the precursor, respectively.

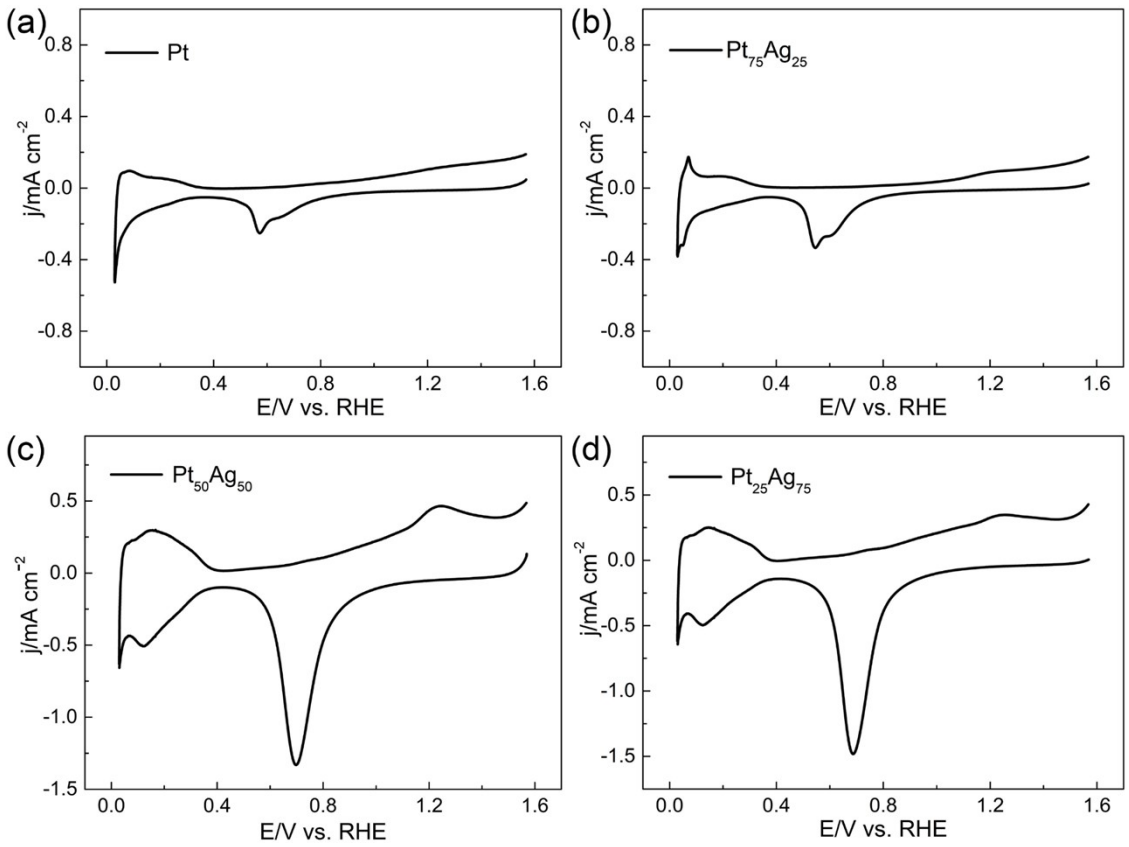

Figure S 6 Cyclic voltammetry (CV) profiles of as-prepared samples in 0.1 M $HClO_4$ solution at a scan rate of 50 mV s^{-1}. (a) Pt NP s, (b) $Pt_{75}Ag_{25}$ NP. (c) $Pt_{50}Ag_{50}$ NP, (d) $Pt_{25}Ag_{75}$ NP.

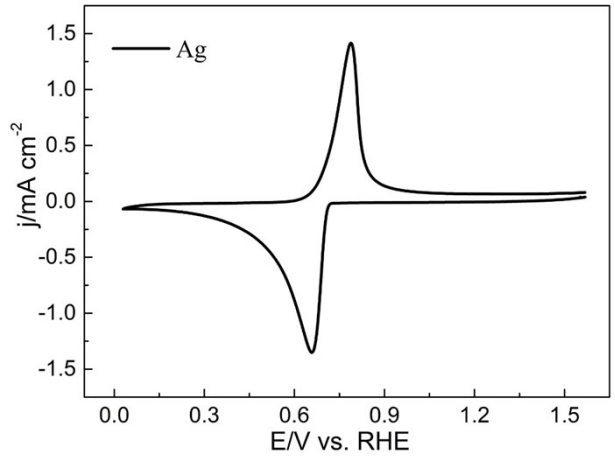

Figure S 7 Cyclic voltammetry(CV) profiles of Ag NP in 0.1 M $HClO_4$ solution at a scan rate of 50 mV s^{-1}.

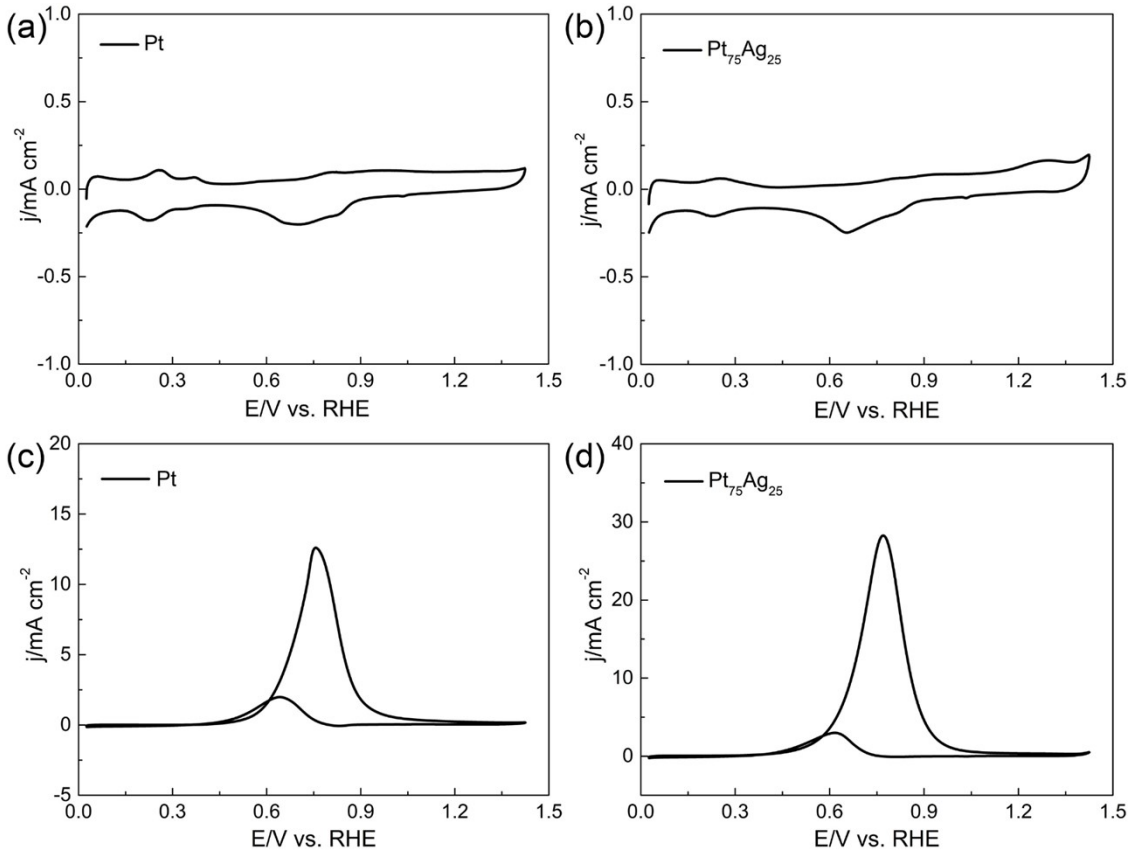

Figure S 8(a, b) Cyclic voltammetry profiles of Pt and $Pt_{75}Ag_{25}$ nanoparticles in 1 M KOH solution. (c, d) Cyclic voltammetry profiles during methanol oxidation reaction for Pt and $Pt_{75}Ag_{25}$nanoparticles in 1 M methanol and 1 M KOH solution. All graphs are at a scan rate of 50 mV s^{-1}.

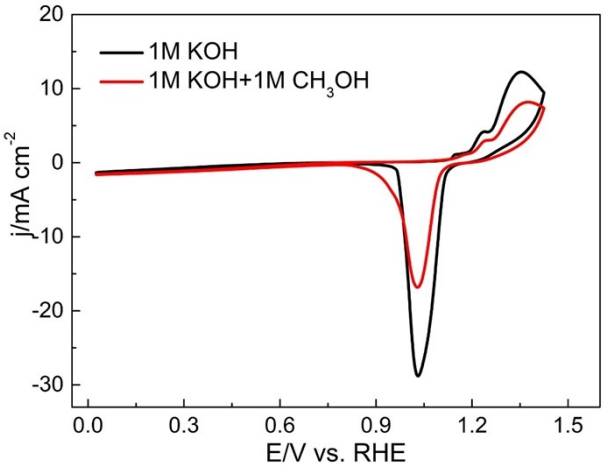

Figure S 9 Cyclic voltammetry (CV) profiles of Ag NP in 1 M KOH solution (black) and in 1 M methanol + 1 M KOH solution (red) at a scan rate of 50 mV s^{-1}.

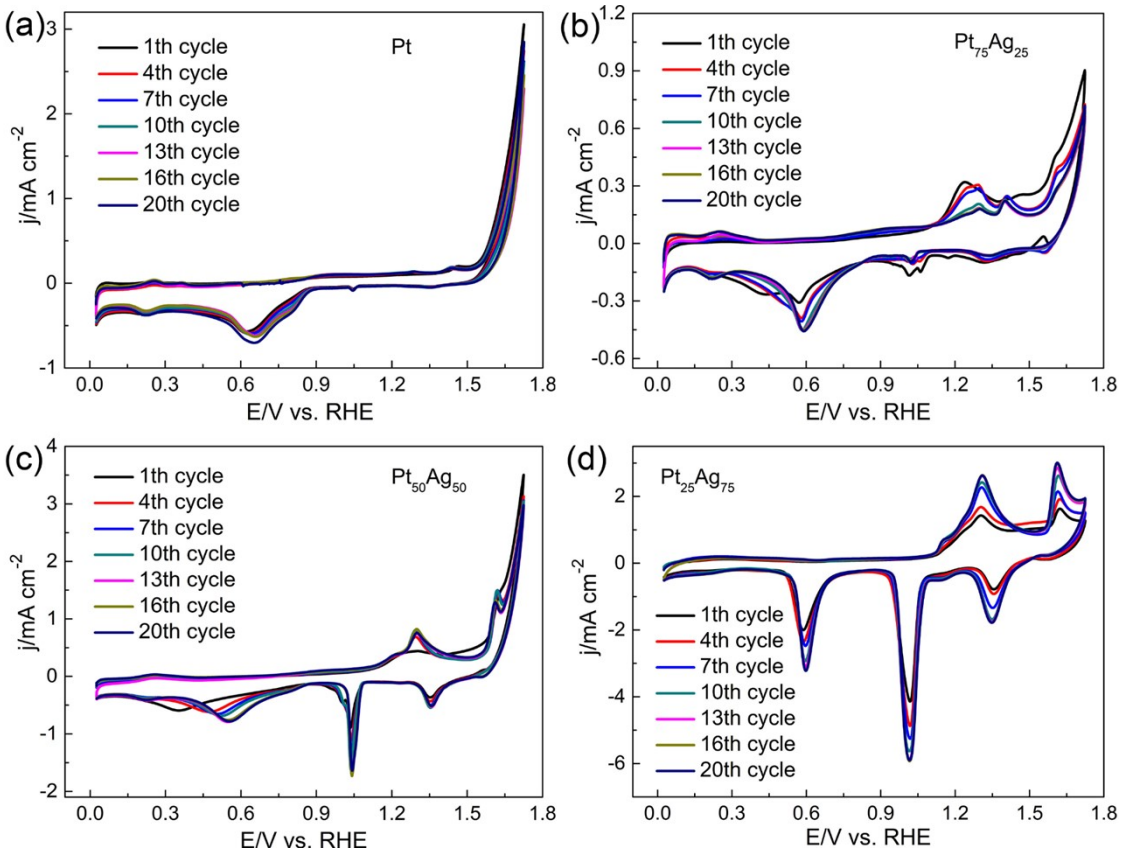

Figure S 10 Cyclic voltammetry profiles of as-prepared samples in 1 M KOH solution at a scan rate of 50 mV s^{-1}. (a) Pt NP, (b) $Pt_{75}Ag_{25}$ NP. (c) $Pt_{50}Ag_{50}$ NP, (d) $Pt_{25}Ag_{75}$ NP.

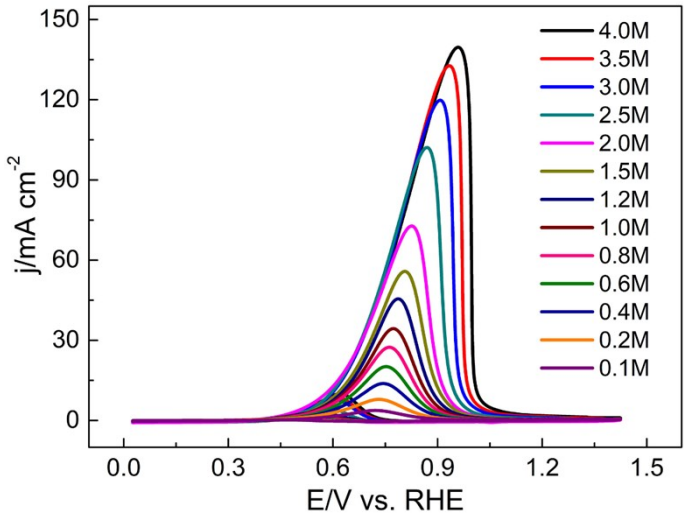

Figure S11 Cyclic voltammetry profiles of methanol oxidation reaction(MOR) for $Pt_{50}Ag_{50}$ NP 1 M KOH solution containing methanol of various concentrations at a scan rate of 50 mV s^{-1}.

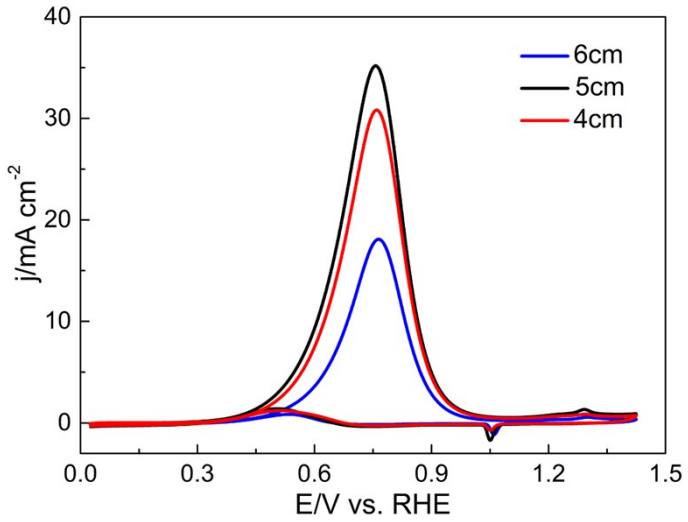

Figure S12 Cyclic voltammetry profiles of methanol oxidation reaction (MOR) for $Pt_{50}Ag_{50}$ NP with different substrate-target distance in 1 M methanol + 1 M KOH solution at a scan rate of 50 mV s^{-1}.

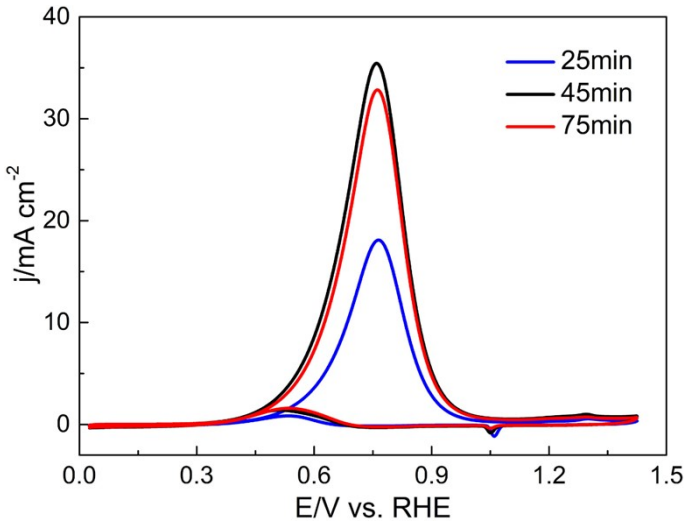

Figure S13 Cyclic voltammetry profiles of methanol oxidation reaction (MOR) for $Pt_{50}Ag_{50}$ NP with different deposition time in 1 M methanol + 1 M KOH solution at a scan rate of 50mV s^{-1}.

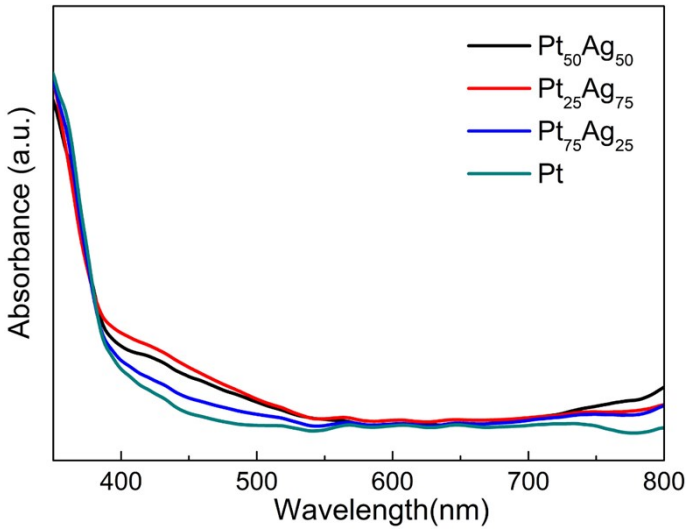

Figure S14 Diffuse reflectance UV-vis absorption spectroscopy of Pt, $Pt_{75}Ag_{25}$, $Pt_{50}Ag_{50}$ and $Pt_{25}Ag_{75}$ NP.

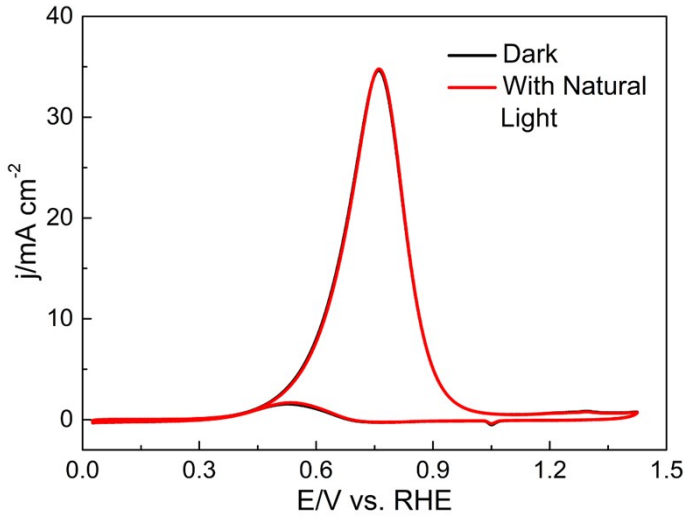

Figure S15 Effect of the natural light on methanol oxidation reaction of $Pt_{50}Ag_{50}$ NP in 1 M methanol + 1 M KOH solution at a scan rate of 50 mV s^{-1}.

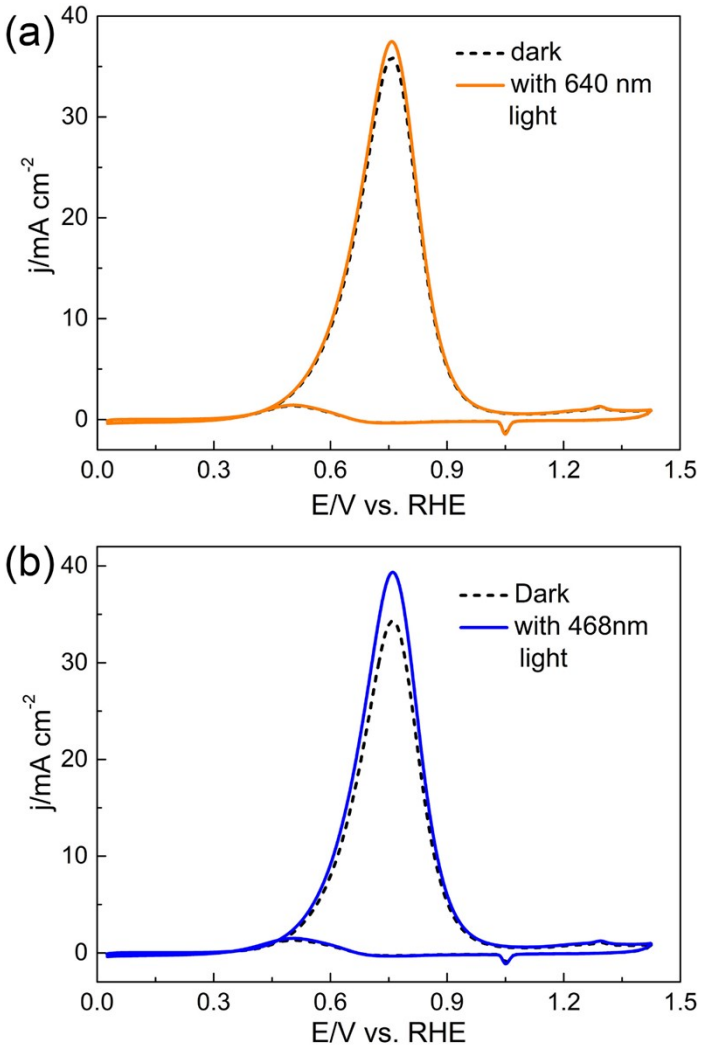

Figure S16 Effect of the UV light of 640 nm and 468 nm on methanol oxidation reaction of $Pt_{50}Ag_{50}$ NP in 1 M methanol + 1 M KOH solution at a scan rate of 50 mV s^{-1}.

Table S1. The elemental compositions obtained by EDX and XPS analysis for three different PtAg catalysts synthesized by PLD.

Catalyst	EDX analysis ［at%］		XPS analysis ［at%］	
	Ag	Pt	Ag	Pt
$Pt_{75}Ag_{25}$	23.16	76.84	24.78	75.22
$Pt_{50}Ag_{50}$	51.55	48.45	53.79	46.21
$Pt_{25}Ag_{75}$	76.41	23.59	79.87	20.13

Table S2. Performance parameters in terms of mass activity, ratio of forward/backward anodic peak current density (I_f/I_b).

Catalyst	Electrolyte concentration(M)	Methanol concentration(M)	Scan rate (mVs^{-1})	Current density ($Amg^{-1}Pt$)	I_f/I_b	Ref.
Pt NP	1	1	50	0.89	6.4	This work
$Pt_{75}Ag_{25}$ NP	1	1	50	1.7	9.5	This work
$Pt_{50}Ag_{50}$ NP	1	1	50	3.6	20.7	This work
$Pt_{25}Ag_{75}$ NP	1	1	50	2.97	7.4	This work
PtC	0.2	1	50	0.351	7.4	[1]
AgAu@Pt	0.2	1	50	0.4831	34.3	[1]
Pt-Ag/C	1	1	50	4.3482	5.65	[2]
Pt-Ag/G	1	1	50	5.6283	—	[2]
Pt-Ag/C	0.5	0.5	50	—	10.67	[3]
Pt-Bi/GNs	1	1	50	2	—	[4]
p-Pt_1Cu_1/AP-GNP	0.1	0.5	50	3.61	10.44	[5]
PdPt/CNTs	0.5	0.5	50	1.10	4.23	[6]
Pt/G_3DN	1	1	50	0.91	3.08	[7]
Pt/P-Ni	1	0.5	100	1.38	—	[8]
Pd_1Pt_1NWs	0.5	0.5	50	—	1.83	[9]
Graphene-Pt NP hybrid	0.1	0.5	10	1.18	4.03	[10]
Au_1Pt_3	0.5	0.5	50	0.1335	—	[11]
Co_3Pt	1	1	50	—	12.1	[12]
Pt/carst-Ni	1	1	20	—	6.25	[13]
Fe_3O_4@CeO_2/Pt-20%	0.5	1	50	0.273	4.5	[14]
PtAuRu/RGO/GC	1	1	50	1.6505	—	[15]
PtCu NFs	0.5	1	50	2.26	2.7	[16]
Pd@Pt/RGO	0.5	0.5	50	4.972	—	[17]

References

1. X. Yan, S. Yu, Y. Tang, D. Sun, L. Xu and C. Xue, *Nanoscale*, 2018, **10**, 2231-2235.
2. A. Shafaei Douk, H. Saravani and M. Noroozifar, *International Journal of Hydrogen Energy*, 2018, **43**, 7946-7955.
3. B. Ruiz-Camacho, R. Morales-Rodriguez and A. Medina Ramírez, *International Journal of Hydrogen Energy*, 2016, **41**, 23336-23344.
4. Z. Li, S. Xu, Y. Xie, Y. Wang and S. Lin, *Electrochimica Acta*, 2018, **264**, 53-60.
5. G. Zhang, Z. Yang, W. Zhang and Y. Wang, *Journal of Materials Chemistry A*, 2016, **4**, 3316-3323.
6. G. Yang, Y. Zhou, H. B. Pan, C. Zhu, S. Fu, C. M. Wai, D. Du, J. J. Zhu and Y. Lin, *Ultrason Sonochem*, 2016, **28**, 192-198.
7. M. Wang, X. Song, Q. Yang, H. Hua, S. Dai, C. Hu and D. Wei, *Journal of Power Sources*, 2015, **273**, 624-630.
8. X. T. Li, H. Lei, C. Yang and Q. B. Zhang, *Journal of Power Sources*, 2018, **396**, 64-72.
9. J.-X. Tang, Q.-S. Chen, L.-X. You, H.-G. Liao, S.-G. Sun, S.-G. Zhou, Z.-N. Xu, Y.-M. Chen and G.-C. Guo, *Journal of Materials Chemistry A*, 2018, **6**, 2327-2336.
10. M. Ayán-Varela, R. Ruiz-Rosas, S. Villar-Rodil, J. I. Paredes, D. Cazorla-Amorós, E. Morallón, A. Martínez-Alonso and J. M. D. Tascón, *Electrochimica Acta*, 2017, **231**, 386-395.
11. Z. Li and Q. Niu, *ACS Sustainable Chemistry & Engineering*, 2013, **2**, 533-536.
12. A. Serrà, E. Gómez, I. Golosovsky, J. Nogues and E. Vallés, *Journal of Materials Chemistry A*, 2016, **4**, 7805-7814.
13. C.-S. Chen, F.-M. Pan and H.-J. Yu, *Applied Catalysis B: Environmental*, 2011, **104**, 382-389.
14. Q. Wang, Y. Li, B. Liu, Q. Dong, G. Xu, L. Zhang and J. Zhang, *Journal of Materials Chemistry A*, 2015, **3**, 139-147 .
15. F. Ren, C. Wang, C. Zhai, F. Jiang, R. Yue, Y. Du, P. Yang and J. Xu, *Journal of Materials Chemistry A*, 2013, **1**, 7255-7261.
16. Z. Zhang, Z. Luo, B. Chen, C. Wei, J. Zhao, J. Chen, X. Zhang, Z. Lai, Z. Fan, C. Tan, M. Zhao, Q. Lu, B. Li, Y. Zong, C. Yan, G. Wang, Z. J. Xu and H. Zhang, *Adv Mater*, 2016, **28**, 8712-8717.
17. Y. Kim, Y. Noh, E. J. Lim, S. Lee, S. M. Choi and W. Bae Kim, *Journal of Materials Chemistry A*, 2014, **2**, 6976-6986 .